Chemistry Research Journal, 2021, 6(4):116-131

Available online www.chemrj.org

Research Article

ISSN: 2455-8990
CODEN(USA): CRJHA5

A DFT study of the relationships between electronic structure and dopamine D_1 and D_2 receptor affinity of a group of (S)-enantiomers of 11-(1,6-dimethyl-1,2,3,6-tetrahydropyridin-4-yl)-5*H*-dibenzo[b,e][1,4]diazepines

Juan S. Gómez-Jeria*, Alonso Ibertti-Arancibia

Quantum Pharmacology Unit, Department of Chemistry, Faculty of Sciences, University of Chile. Las Palmeras 3425, Santiago 7800003, Chile
*Corresponding author: Juan S. Gómez-Jeria

Abstract A Density Functional Theory study was carried out to obtain quantitative relationships between the electronic structure of a group of (S)-enantiomers of 11-(1,6-dimethyl-1,2,3,6-tetrahydropyridin-4-yl)-5*H*-dibenzo[b,e][1,4]diazepines and their dopamine receptor affinity (D_1 and D_2 receptors). For both receptors statistically significant equations were found. From these equations the corresponding partial 2D pharmacophores were built. Some possible atom-site interactions are proposed as well as some possible substitutions to modify receptor affinity.

Keywords Dopamine receptors, dopamine D_1 receptor, dopamine D_2 receptor, Density Functional Theory, receptor affinity, Klopman-Peradejordi-Gómez method, QSAR, KPG method, local atomic reactivity indices, diazepines, schizophrenia

Introduction

Schizophrenia is a very complex disorder in both its causes and its symptoms. This illness, affecting nearly 1% of the population worldwide, has been studied for about 140 years [1]. Schizophrenia is a serious mental illness involving changes in thought, patterns, emotions, behaviors, and ways of observing the outside world. Schizophrenia is probably not one disorder, but a range of related disorders that vary in symptoms, severity, and outcome [1]. Following the National Institute of Mental Health the symptoms of schizophrenia generally fall into the following three categories: psychotic symptoms (hallucinations, delusions, thought disorder), negative symptoms (reduced speaking, reduced expression of emotions via facial expression or voice tone, diminished feelings of pleasure in everyday life, reduced motivation and difficulty planning, beginning, and sustaining activities) and cognitive symptoms (difficulty processing information to make decisions, problems using information immediately after learning it, trouble focusing or paying attention) (taken from https://www.nimh.nih.gov/health/topics/schizophrenia). The causes of schizophrenia are not entirely understood. For this reason, some of the current treatments make emphasis on managing symptoms. Antipsychotic drugs are the backbone of therapeutic intervention. Nevertheless, about 30% of patients are categorized as treatment-resistant schizophrenia (TRS). TRS is defined as the persistence of positive symptoms despite 2 or more trials of satisfactory dose and duration of antipsychotic medication with documented adherence [2-7]. For these patients, doctors prescribe the atypical antipsychotic clozapine as medication [8-13]. Clozapine binds to serotonin, dopamine and $GABA_B$ receptors but its exact mechanism of actions is not

known [4, 6, 11, 14-18]. Several derivatives of clozapine have been synthesized and tested [19-29]. Recently, Watanabe et al. analyzed a group of 11-(1,6-dimethyl-1,2,3,6-tetrahydropyridin-4-yl)-5H-dibenzo[b,e][1,4]diazepines. They reported experimental data of dopamine D_1 and D_2 receptors affinities [30]. Here we report the results of a quantum-chemical study searching for quantitative relationships between the electronic structure of the abovementioned molecules and their dopamine receptor affinities.

Methods, Models and Calculations [31]

The Method

Our technique to find physically-based structure-activity relationships is based on the ensuing ideas [31]. A model to analyze the affinity constant is proposed starting from the statistical-mechanical definition. Next, scientifically-based approximations are employed to transform the model into mathematical equations. This approach was successfully applied to several kinds of receptors and molecules. The next stage was to enlarge the original equation with about fifteen more members. Finally, this method was generalized to any biological activity (BA). The final result is the following system of n linear equations (for n molecules) [32-44]:

$$\log(BA)_i = a + bM_{D_i} + c\log\left[\sigma_{D_i}/(ABC)^{1/2}\right] + \sum_{j=1}^{E}\left[e_jQ_j + f_jS_j^E + s_jS_j^N\right]$$
$$+\sum_{j=1}^{E}\sum_{m=(HOMO-2)^*}^{(HOMO)^*}\left[h_j(m)F_j(m) + x_j(m)S_j^E(m)\right] + \sum_{j=1}^{E}\sum_{m'=(LUMO)^*}^{(LUMO+2)^*}\left[r_j(m')F_j(m') + t_j(m')S_j^N(m')\right]$$
$$+\sum_{j=1}^{E}\left[g_j\mu_j + k_j\eta_j + o_j\omega_j + z_j\varsigma_j + w_jQ_j^{max}\right] \quad (i=1,\ldots,n) \qquad (1)$$

where BA is the biological activity, M is the drug's mass, σ its symmetry number, ABC the product of the drug's moments of inertia about the three principal axes of rotation, Q_i is the net charge of atom *i*, S_i^E and S_i^N are, respectively, the total atomic electrophilic and nucleophilic superdelocalizabilities of Fukui et al., $F_{i,m}$ is the electron population of atom i in occupied (empty) MO (molecular orbital) m (m'). $S_i^E(m)$ is the electrophilic superdelocalizability of atom i in occupied MO m, $S_i^E(m')$ is the nucleophilic superdelocalizability of atom i in empty MO m'. μ_j, η_j, ω_j, ς_j and Q_j^{max} are, respectively, the local atomic electronic chemical potential of atom j, the local atomic hardness of atom j, the local atomic electrophilicity of atom j, the local atomic softness of atom j and the maximal amount of electronic charge that atom j may accept. These local atomic reactivity indices (LARIs) are expressed in eV like the global ones and not in eV·e as are the projected local reactivity indices coming from Density Functional Theory [40]. The summation on atoms runs from one to E. E corresponds to the so called common skeleton (CS, see below).The summation on the occupied molecular orbitals goes from (HOMO-2)* to (HOMO)* and that the summation on empty MOs runs from (LUMO)* to (LUMO+2)* (with an asterisk). They are called the local molecular orbitals of a given atom. Let be Ã the set of all occupied MOs of a molecule. The set of local molecular orbitals of atom f is defined as the subset of Ã comprising all MOs having an electron population on f equal or greater than 0.1 e [40]. We are working with only the three highest occupied local MOs and the three lowest empty local MOs for the atoms considered in E. This method is called the Klopman-Peradejordi-Gómez approach (KPG).

Selection of molecules and biological activities

The molecules are a group of (S)-enantiomers of diazepine derivatives selected from a recent study [30]. Their general formula and dopamine D_1 and D_2 receptor affinity are displayed, respectively, in Fig. 1 and Table 1. The dopamine D_1 receptor affinity was evaluated in CHO cells expressing human D_1 receptor, with ^{3}H-SCH23390 as radioligand and SCH23390 as displacer. The dopamine D_2 receptor affinity was evaluated in CHO cells expressing human D_2 receptor with ^{3}H-Spiperone as radioligand and spiperone as displacer. The reported K_i values were

calculated with the equation $K_i = IC_{50}/(1 + S/K_d)$, where S is the radioligand concentration used in the assay and K_d is the dissociation constant.

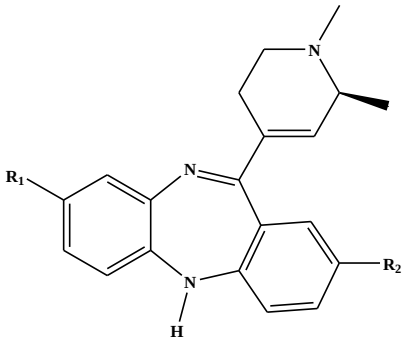

Figure 1: General formula of the (S)-enantiomers of diazepine derivatives

Table 1: (S)-enantiomers of diazepine derivatives and dopamine D_1 and D_2 receptor affinities

Molecule	R_1	R_2	$\log(K_i)$ D_1	$\log(K_i)$ D_2
1	Cl	H	1.71	2.68
2	Cl	Me	0.36	1.8
3	Cl	Et	0.15	1.45
4	Cl	OMe	0.3	1.84
5	Cl	OEt	0.57	1.67
6	Cl	OCF3	0.3	2.04
7	Cl	F	-0.7	2.1
8	Cl	Cl	-0.046	2.02
9	Cl	CN	0.041	2.13
10	Me	OCF3	0.38	3.09
11	Me	F	0.74	2.66
12	Me	Cl	-0.32	1.99
13	H	Me	0.9	2.91
14	H	Et	0.6	2.22
15	H	Cl	0.2	2.09

Figures 2 and 3show graphical representations of the D_1 experimental data employed here. Figure 2 shows a histogram of frequencies with the percentage of observations in the upper part of each rectangle (percentages add up to more than 100% due to the use of integer numbers).

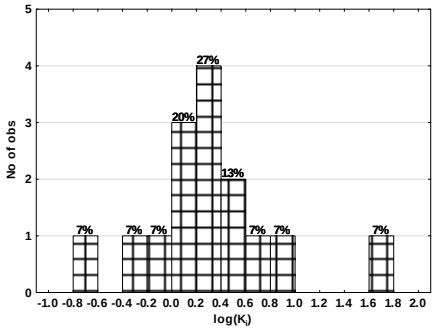

Figure 2: Histogram of the frequencies of the D_1 receptor affinity data

We can see that more than 50% of the data is between $\log(K_i)$ values of -0.4 and 1.0. The gap between groups of data at the right side of the plot is originated only because no molecules presented values of D_1 receptor affinity data within this range. Figure 3 shows the Box-Whiskers plot of the D_1 data values with median and quartile values.

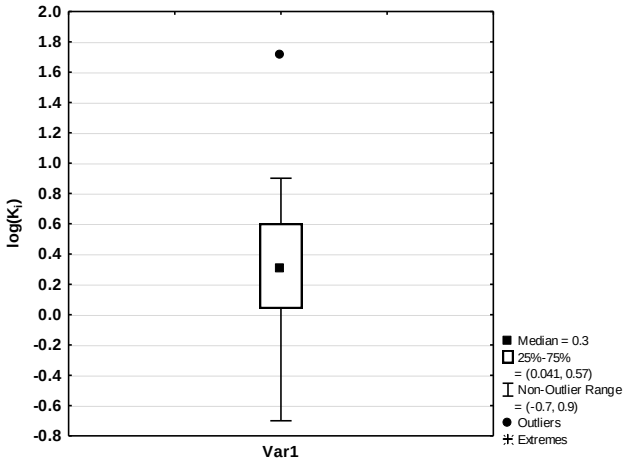

Figure 3: Median/Quart./Range Box-Whiskers plot of the D_1 receptor affinity data

We can see that perhaps an outlier exists. Because we have no reasons to question experimental results, we include this outlier in the data matrix. Moreover, it seems that this outlier appears due only to the absence of $\log(K_i)$ data between 0.9 and 1.71 (see Table 1). Figures 4 and 5 show graphical representations of the D_2 receptor affinity experimental data employed here.

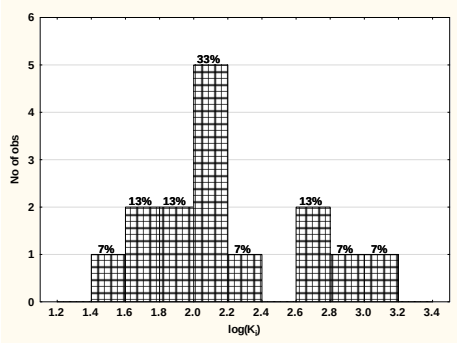

Figure 4: Histogram of the frequencies of the D_2 receptor affinity data

We can see that the distribution of data is almost continuous and that about one third of the date is between values of $\log(K_i)$ of 2.0 and 2.2.

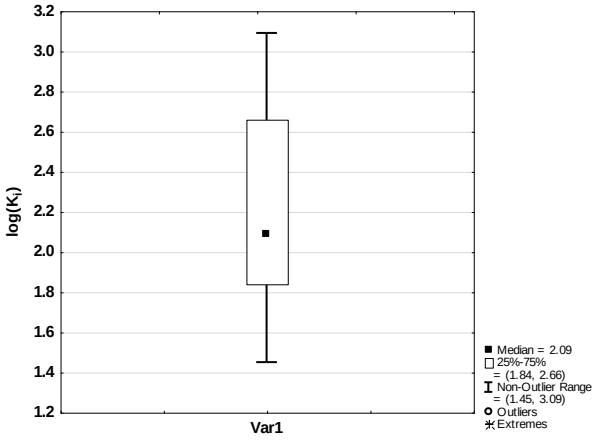

Figure 5: Median/Quart./Range Box-Whiskers plot of the D_2 receptor affinity data

We can see that no outliers or extreme data exist.

Calculations

The electronic structure of all molecules was calculated within the Density Functional Theory (DFT) at the B3LYP/6-31G(d,p) level with full geometry optimization. The Gaussian suite of programs was used [45]. All the information needed to calculate numerical values for the local atomic reactivity indices was obtained from the Gaussian results with the D-Cent-QSAR software [46]. All the electron populations smaller than or equal to 0.01 e were considered as zero. Negative electron populations coming from Mulliken Population Analysis were corrected as usual [47]. Since the resolution of the system of linear equations is not possible because we have not enough molecules, we made use of Linear Multiple Regression Analysis (LMRA) techniques to find the best solution. For each case, a matrix containing the dependent variable ($\log(K_i)$ of each case) and the local atomic reactivity indices of all atoms of the common skeleton as independent variables was built. The Statistica software was used for LMRA [48].

Because the right side of Eq. 1 needs the same number of terms for all molecules, we have introduced the common *skeleton hypothesis* coming directly from the concept of atom-atom interactions [49]. To build the common skeleton we select E atoms of any of the molecules. These E atoms must have similar counterparts in all the remaining molecules of the set but they do not need to be of the same nature (i.e., a carbon atom in one molecule could be a nitrogen atom or an oxygen atom in another) Therefore the common skeleton of all molecules can be superimposed, implying that these structures must be oriented in the same way in all molecules when exerting their biological activity. It is hypothesized that different parts of this common skeleton account for all or almost all the atom-atom interactions leading to the expression of the biological activity. The action of the remaining atoms is to modify the electronic structure of the common skeleton (they can also bind receptors or other macromolecules) and to influence the right alignment of the drug (throughout the orientational parameters). The common skeleton is shown in Fig. 6.

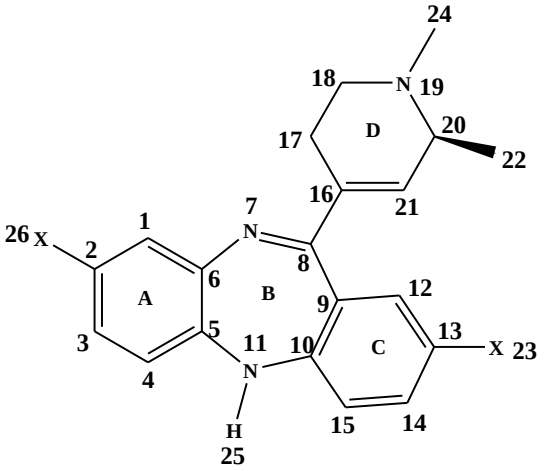

Figure 6: Common skeleton numbering

Results

Concerning the interpretation of the QSAR equations, an important point to stress is the following. When a local atomic reactivity index of an inner occupied local MO ((HOMO-1)* and/or (HOMO-2)*) or of a higher vacant local MO ((LUMO+1)* and/or (LUMO+2)*) appears in any equation, this means that the remaining of the upper occupied local MOs (for example, if (HOMO-2)* appears, upper means (HOMO-1)* and (HOMO)*) or the remaining of the empty local MOs (for example, if (LUMO+1)* appears, lower means the (LUMO)*) contribute to the interaction. Their nonappearance in the equation only means that the variation of their numerical values does not account for the variation of the numerical value of the biological property. Also, it is considered that the absent local MOs behave in the same way that the local MOs appearing into the equations. A second point is the presence of outliers in various equations during the LMRA procedure. Single outliers can significantly change the slope of the

regression line and therefore the value of the correlation. Also, outliers artificially increase the value of a correlation coefficient and also decrease the value of a correlation.

Results for the dopamine D_1 receptor affinity

The best equation obtained was:

$$\log(K_i)=25.49+0.02S_{11}^{N}-1.42S_{19}^{N}-3.82S_{16}^{E}(\mathrm{HOMO})^{*}-17.63F_{15}(\mathrm{HOMO-2})^{*} \quad (2)$$

with n=15, R=0.98, R^2=0.96, adj-R^2=0.94, F(4,10)=58.876 (p<0.00001) and SD=0.13. No outliers were detected and no residuals fall outside the ±2σ limits. Here, S_{11}^{N} is the total atomic nucleophilic superdelocalizability of atom 11, S_{19}^{N} is the total atomic nucleophilic superdelocalizability of atom 19, S_{16}^{E}(HOMO)* is the electrophilic superdelocalizability of the highest occupied local MO of atom 16 and F_{15}(HOMO-2)* is the Fukui index of the third highest occupied local MO of atom 15. Tables 2 and 3 show the beta coefficients, the results of the t-test for significance of coefficients and the matrix of squared correlation coefficients for the variables of Eq. 2. There are no significant internal correlations between independent variables (Table 3). Figure 5 displays the plot of observed *vs.* calculated values.

Table 2: Beta coefficients and t-test for significance of coefficients in Eq. 2

Variable	Beta	t(10)	p-level
S_{11}^{N}	1.06	15.15	0.000000
S_{19}^{N}	-0.53	-7.45	0.00002
S_{16}^{E}(HOMO)*	-0.23	-3.42	0.007
F_{15}(HOMO-2)*	-0.19	-2.92	0.02

Table 3: Matrix of squared correlation coefficients for the variables in Eq. 2

	S_{11}^{N}	S_{19}^{N}	S_{16}^{E}(HOMO)*	F_{15}(HOMO-2)*
S_{11}^{N}	1			
S_{19}^{N}	0.08	1		
S_{16}^{E}(HOMO)*	0.03	0.07	1	
F_{15}(HOMO-2)*	0.02	0.02	0.0004	1

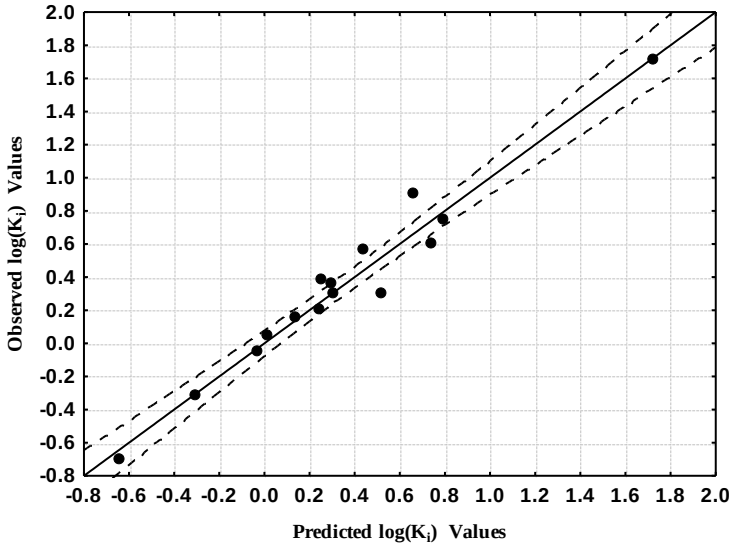

Figure 7: Plot of predicted vs. observed log(K_i) values (Eq. 2). Dashed lines denote the 95% confidence interval

The associated statistical parameters of Eq. 2 indicate that this equation is statistically significant and that the variation of the numerical values of a group of four local atomic reactivity indices of atoms constituting the common skeleton explains about 94% of the variation of log(K_1). Figure 7, spanning about 2.4 orders of magnitude, shows

that there is a good correlation of observed *versus* calculated values. Figures 8, 9 and 10 show, respectively, the plot of predicted values vs. residuals scores, the plot of residual vs. deleted residuals and the normal probability plot of residuals.

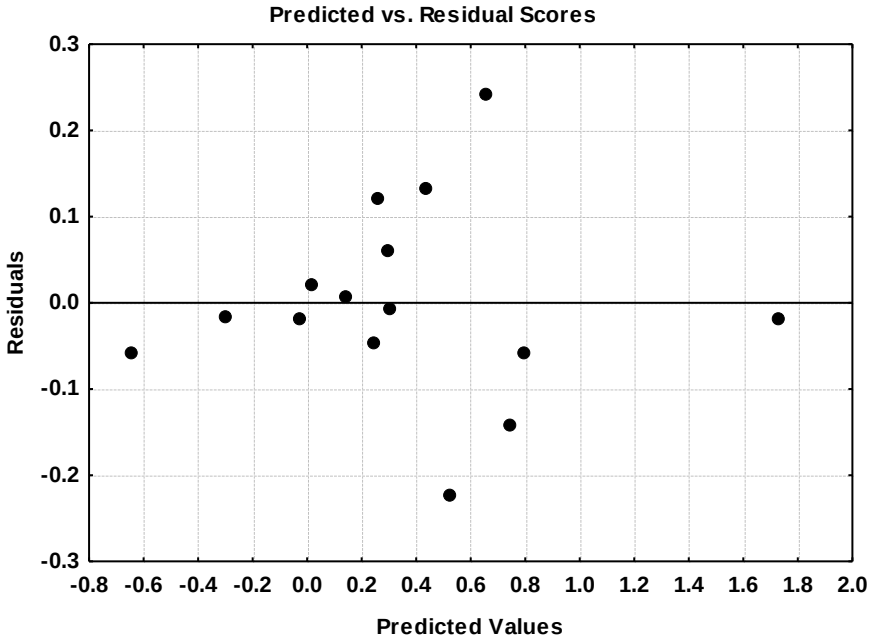

Figure 8: Plot of predicted values vs. residuals scores

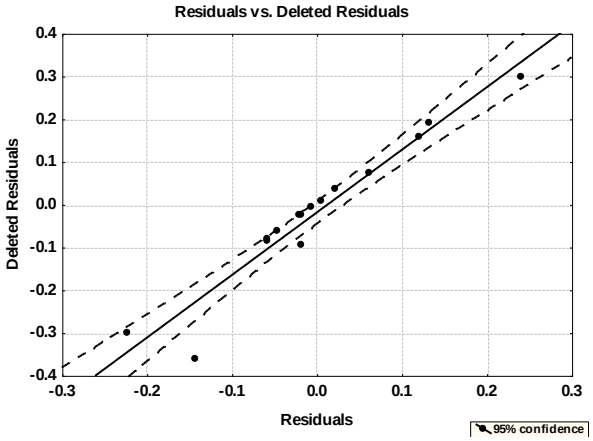

Figure 9: Plot of residual vs. deleted residuals

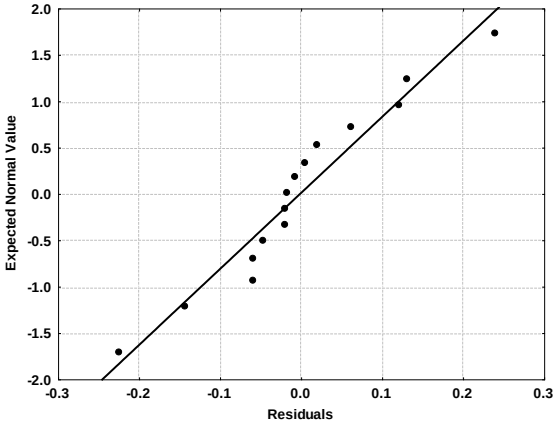

Figure 10: Normal probability plot of residuals

We can see that that there is a general absence of fitting and that the data does not appear to form a determined pattern around the line then the variable does not need be transformed and that our use of a linear model is appropriate. The points should cluster around a straight line for a normally distributed variable. The distribution of points in the three plots shows that the assumption of linearity is a good first approach. Therefore, equation 2 is suitable to be employed for an analysis of the structure-affinity relationships.

Results for the dopamine D_2 receptor affinity

During the LRMA analysis only one data appeared as being an outlier and was removed from the set. The best equation was:

$$\log(K_i)=1.04+7.00F_{25}(\text{LUMO})^*+42.12F_{22}(\text{LUMO+1})^*+$$
$$+0.002S_{10}^{N}(\text{LUMO+2})^*-2.24F_{12}(\text{HOMO})^* \quad (3)$$

with n=14, R=0.96, R^2=0.93, adj-R^2=0.89, F(4,9)=27.250 (p<0.00005) and SD=0.14. No outliers were detected and no residuals fall outside the ±2σ limits. Here, F_{25}(LUMO)* is the Fukui index of the lowest empty local MO of atom 25, F_{22}(LUMO+1)* is the Fukui index of the second lowest empty local MO of atom 22, S_{10}^{N}(LUMO+2)* is the nucleophilic superdelocalizability of the third lowest empty local MO of atom 10 and F_{12}(HOMO)* is the Fukui index of the highest occupied local MO of atom 12.Tables 4 and 5 show the beta coefficients, the results of the t-test for significance of coefficients and the matrix of squared correlation coefficients for the variables of Eq. 3. There are no significant internal correlations between independent variables (Table 5). Figure 11 displays the plot of observed *vs.* calculated values.

Table 4: Beta coefficients and t-test for significance of coefficients in Eq. 3

Variable	Beta	t(9)	p-level
F_{25}(LUMO)*	0.60	5.77	0.0003
F_{22}(LUMO+1)*	0.73	6.73	0.00009
S_{10}^{N}(LUMO+2)*	0.44	3.69	0.005
F_{12}(HOMO)*	-0.23	-2.41	0.04

Table 5: Matrix of squared correlation coefficients for the variables in Eq. 3

	F_{25}(LUMO)*	F_{22}(LUMO+1)*	S_{10}^{N}(LUMO+2)*	F_{12}(HOMO)*
F_{25}(LUMO)*	1			
F_{22}(LUMO+1)*	0.02	1		
S_{10}^{N}(LUMO+2)*	0.17	0.26	1	
F_{12}(HOMO)*	0.04	0.01	0.0001	1

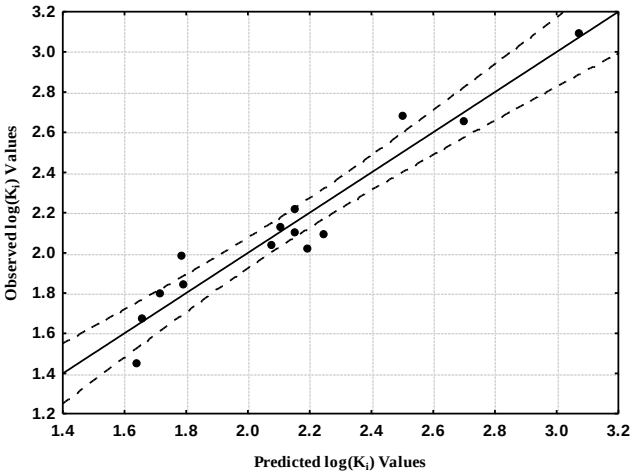

Figure 11: Plot of predicted vs. observed log(K_i) values (Eq. 3). Dashed lines denote the 95% confidence interval

The associated statistical parameters of Eq. 3 indicate that this equation is statistically significant and that the variation of the numerical values of a group of four local atomic reactivity indices of atoms constituting the common skeleton explains about 89% of the variation of log(K_i). Figure 11, spanning about 1.5 orders of magnitude, shows that there is a relatively good correlation of observed *versus* calculated values. Figures 11, 12 and 13 show, respectively, the plot of predicted values vs. residuals scores, the plot of residual vs. deleted residuals and the normal probability plot of residuals (Eq. 3).

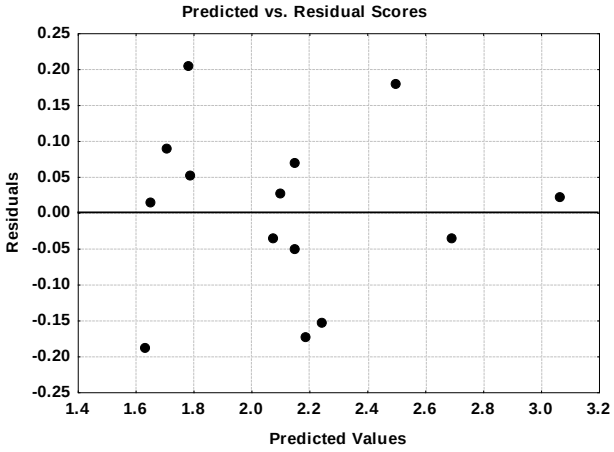

Figure 11: Plot of predicted values vs. residuals scores

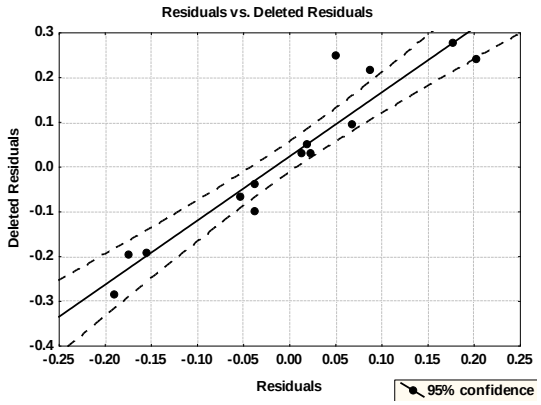

Figure 12: Plot of residual vs. deleted residuals

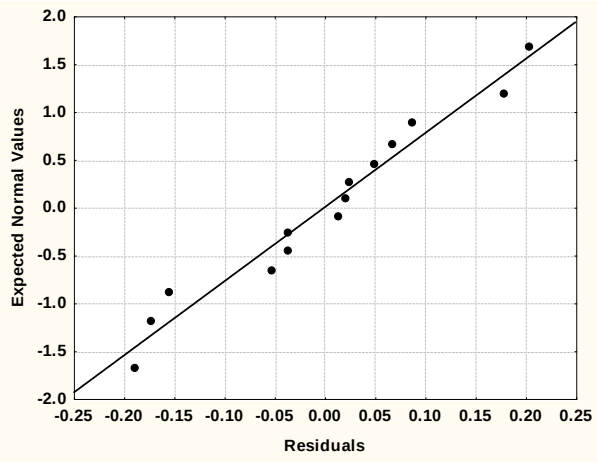

Figure 13: Normal probability plot of residuals

We can see that the points cluster around a straight line. The distribution of points in these three plots shows that the assumption of linearity is a good first approach. Therefore, equation 3 is also appropriate to deal with the structure-affinity relationships.

Local Molecular Orbitals

Tables 6 and 7 show the local MO structure of atoms 10, 11, 12, 16, 19, 22 and 25 (see Fig. 6). Nomenclature: Molecule (HOMO) / (HOMO-2)* (HOMO-1)* (HOMO)* - (LUMO)* (LUMO+1)* (LUMO+2)*.

Table 6: Local molecular orbitals of atoms 10, 11, 12 and 15

Mol.	Atom 10	Atom 11	Atom 12	Atom 15
1(89)	86π87π89π- 90σ91π92σ	87σ88σ89σ- 92σ93σ94σ	85σ86π87π- 90π91σ92π	86π87π89π- 90π91σ92π
2(93)	90π91π93π- 94π95π96σ	91σ92π93σ- 96σ97σ98σ	89σ90π91π- 94π95σ96π	90π91π93π- 94π95σ96π
3(97)	94π95π97π- 98π99π100σ	95σ96σ97σ- 100π101σ102σ	93σ94π95π- 98π99σ100π	94π95π97π- 98π99σ100π
4(97)	94π95π97π- 98π99π100π	94σ95σ97σ- 100σ101σ102σ	93σ94π95π- 98π99σ100σ	94π95π97π- 98π99σ100σ
5(101)	98π99π101π- 102π103π104π	98σ99σ101σ- 104σ105σ106σ	98π99π101π- 102π103σ104σ	98π99π101π- 102π103σ104σ
6(109)	107π108σ109π- 110π111π112σ	107σ108σ109σ- 112σ113σ114σ	105σ106π107π- 110π111σ112π	107π108σ109π- 110π111σ112π
7(93)	90π91π93π- 94π95π96σ	91σ92σ93σ- 97σ98σ105σ	89σ90π91π- 94π95σ96π	90π91π93π- 94π95π96π
8(97)	95π96σ97π- 98π99π100σ	95σ96σ97σ- 100σ101σ102σ	93σ94π95π- 98π99σ100π	94π95π97π- 98π99σ100π
9(95)	92π93σ94π- 96π97σ98σ	93σ94σ95σ- 97σ99σ100σ	91π92π93π- 96π97σ98π	92π93π94π- 96π97π98σ
10(105)	102π103π105π- 106π107π108σ	103σ104σ105σ- 108σ109σ110σ	101π102π103π- 106π107σ108π	102π103π105π- 106π107σ108π
11(89)	86π87π89π- 90π91π92σ	86σ87σ89σ- 92σ93σ94σ	85σ86π87π- 90π91σ92π	85σ87π89π- 90π91σ92π
12(93)	90π91π93π- 94π95π96σ	91σ92σ93σ- 96σ97σ98σ	89σ90π91π- 94π95σ96π	90π91π93π- 94π95σ96π
13(85)	82π83π85π-	78σ83σ85σ-	81σ82π83π-	82π83π85π-

	86π87π88σ	88σ89σ90σ	86π87σ88π	86π87σ88π
14(89)	86π87π89π-90π91π92σ	82σ87σ89σ-92σ93σ94σ	85σ86π87π-90π91σ92π	86π87π89π-90π91σ92π
15(89)	86π87π89π-90π91π92σ	87σ88σ89σ-92σ93σ94σ	85σ86π87π-90π91σ92π	86π87π89π-90π91σ92π

Table 7: Local molecular orbitals of atoms 16, 19, 22 and 25

Mol.	Atom 16	Atom 19	Atom 22	Atom 25
1(89)	86σ87π89π-90σ91σ92σ	87σ88σ89σ-100σ102σ103σ	85σ88σ89σ-94σ100σ103σ	66σ75σ78σ-95σ96σ97σ
2(93)	89π91π93π-94σ95σ96σ	91σ92σ93σ-104σ106σ107σ	89σ92σ93σ-98σ104σ105σ	80σ82σ86σ-99σ100σ101σ
3(97)	93π95π97π-98σ99π100σ	95σ96σ97σ-109σ110σ112σ	93σ96σ97σ-102σ109σ110σ	72σ81σ90σ-103σ104σ106σ
4(97)	94π95π97π-98σ99σ100σ	88σ95σ96σ-109σ111σ112σ	88σ93σ96σ-109σ112σ116σ	80σ83σ84σ-103σ104σ105σ
5(101)	98π99π101π-102σ103π104σ	92σ99σ100σ-113σ115σ116σ	92σ97σ100σ-113σ114σ117σ	85σ87σ88σ-107σ108σ109σ
6(109)	105π107π109π-110σ111π112π	107σ108σ109σ-120σ122σ123σ	107σ108σ109σ-114σ120σ123σ	81σ93σ95σ-115σ116σ117σ
7(93)	89π91π93π-94σ95π97π	91σ92σ93σ-104σ106σ107σ	91σ92σ93σ-98σ104σ107σ	79σ82σ86σ-97σ99σ100σ
8(97)	93π95π97π-98σ99π100π	95σ96σ97σ-109σ111σ112σ	95σ96σ97σ-102σ109σ112σ	72σ82σ83σ-103σ104σ106σ
9(95)	93π94π95σ-96σ97σ98π	93σ94σ95σ-108σ110σ111σ	92σ93σ95σ-100σ108σ111σ	70σ78σ79σ-101σ103σ104σ
10(105)	102π103π105π-106σ107π108π	103σ104σ105σ-116σ117σ118σ	102σ104σ105σ-110σ116σ119σ	87σ88σ98σ-111σ112σ113σ
11(89)	85π87π89π-90σ91π92π	81σ87σ88σ-100σ101σ102σ	81σ85σ88σ-100σ102σ103σ	75σ78σ82σ-95σ96σ97σ
12(93)	89π91π93π-94σ95π96π	91σ92σ93σ-104σ105σ106σ	89σ92σ93σ-105σ108σ111σ	77σ81σ86σ-99σ101σ102σ
13(85)	81π83π85π-86σ87π88π	77σ83σ84σ-96σ98σ99σ	77σ81σ84σ-96σ97σ99σ	65σ74σ78σ-91σ92σ94σ
14(89)	85π87π89π-90σ91π92π	81σ87σ88σ-100σ102σ103σ	81σ85σ88σ-100σ102σ103σ	67σ76σ82σ-95σ96σ97σ
15(89)	85π87π89π-90σ91π92π	87σ88σ89σ-100σ101σ102σ	85σ88σ89σ-94σ101σ103σ	73σ77σ82σ-95σ96σ97σ

Discussion

Discussion of D_1 receptor affinity results

Table 2 shows that the importance of variables in Eq. 2 is S_{11}^N>> S_{19}^N> S_{16}^E(HOMO)*> F_{15}(HOMO-2)*.A variable-by-variable analysis of Eq. 2 shows that a high D_1 receptor affinity is associated with low numerical values for S_{11}^N (positive) and S_{16}^E(HOMO)* (negative); and with high positive numerical values for S_{19}^N andF_{15}(HOMO-2)*.Atom 11 is a nitrogen atom in ring B (Fig. 6). A high D_1 receptor affinity is associated with small positive numerical values for S_{11}^N. Knowing that all the terms composing this reactivity index have the form of (number of electrons in MO z)/(energy of MO z), it is clear that the ones corresponding to the lowest empty molecular orbitals are the

principal ones. Therefore, if we want to obtain a smaller value for this index we must shift upwards the energies of these MOs. Of course another way of getting the same results is by eliminating the localization of these MOs on atom 11 by appropriate chemical changes. The result is that atom 11 will behave as a bad electron acceptor and also will not interact strongly with electron-rich centers. The results of the full geometry optimization show that in all the molecules atom 11 is not conjugated with rings A and C. This fact is reflected in the fact that all the local OMs of this atom have a sigma character (Table 6).Table 6 also shows that $(HOMO)_{11}^{*}$ coincides with the molecular HOMO in all cases. A reasonable explanation of this last fact in combination with a low electron-accepting capacity suggests that atom 11 could be involved in a classical hydrogen bond of the N-H…O kind. Another possibility is that atom 11 could form a hydrogen bond using its lone pair. To test this possibility the hydrogen atom bonded to N11 could be replaced by a methyl group. Atom 16 is a carbon atom in ring D (Fig. 6). C16 has a double bond with another carbon atom, but the pi electrons are not conjugated with ring B because both rings are not coplanar. A high D1 receptor affinity is associated with a small negative numerical value for S_{16}^{E}(HOMO)*. This value is obtained by shifting the $(HOMO)_{16}^{*}$ energy toward more negative values, making this MO less prone to give electrons or to interact with electron-deficient centers. In the limit situation, we can substitute the common skeleton to avoid the HOMO localization on this atom (i.e., the local HOMO* will coincide with an inner occupied MO). Table 6 shows that $(LUMO)_{16}^{*}$ coincides with the molecular LUMO in all cases and has a sigma nature. These facts suggest that atom 16 is facing an electron-rich center. The nature of the interaction is unclear (σ-π or σ-σ?). Atom 19 is a nitrogen atom in ring D (Fig. 6). Table 7 shows that all local MOs have a sigma nature, that $(HOMO)_{19}^{*}$ coincides with the molecular HOMO in all but two cases and that $(LUMO)_{19}^{*}$ is energetically far from the molecular LUMO. Large positive numerical values for S_{19}^{N} are associated with high receptor affinity. As mentioned in the case of atom 11, there first terms are the main ones. In this case, large values are obtained by shifting the energy of $(LUMO)_{19}^{*}$ toward zero, making it more reactive. We suggest then that this atom is interacting with an electron-rich center. We can test this suggestion by substituting this atom with an electron-withdrawing group. Atom 15 is a carbon atom in ring C (Fig. 6). Table 6 shows that local frontier orbitals have a pi nature in all cases. All empty local molecular orbitals coincide with the molecular LUMO and almost all occupied local MOs coincide with the molecular HOMO (with one exception). A large value of F_{15}(HOMO-2)* value is associated with high D_1 receptor affinity. $(HOMO-2)_{15}^{*}$ has a pi nature in all cases (Table 6). Knowing that the maximal number of electrons in a molecular orbital is 2, the best situation is when this MO is localized only on atom 15. Therefore it is suggested that atom 15 is interacting with an electron-deficient counterpart. All the suggestions are displayed in the partial 2D pharmacophore of Fig. 14.

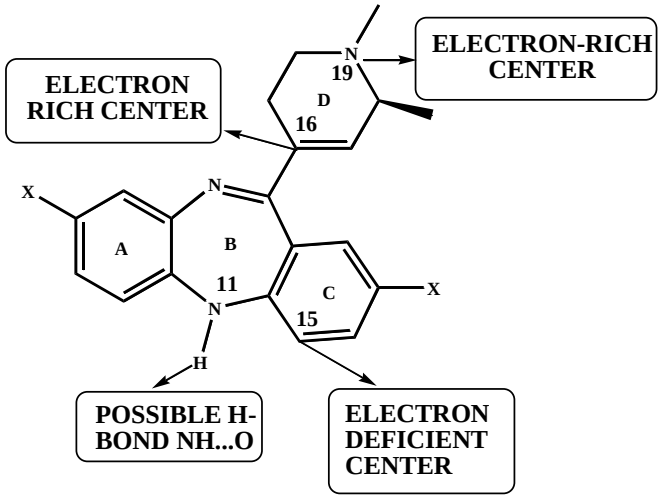

Figure 14: Partial 2D pharmacophore for D_1 receptor affinity

Discussion of D_2 receptor affinity results

Table 4 shows that the importance of variables in Eq. 3 is F_{22}(LUMO+1)*> F_{25}(LUMO)*> S_{10}^{N}(LUMO+2)*> F_{12}(HOMO)*.A variable-by-variable analysis of Eq. 3 shows that a high D_2 receptor affinity is associated with small

numerical values for F_{25}(LUMO)*, F_{22}(LUMO+1)* and S_{10}^{N}(LUMO+2)*; and with large numerical values for F_{12}(HOMO)*.Atom 25 is the hydrogen atom bonded to N11 (Fig. 6). Table 7 shows that all local MOs have a sigma nature. The local $(HOMO)_{25}^{*}$ and local $(LUMO)_{25}^{*}$ are energetically far from the corresponding molecular frontier MOs. The requirement for a high affinity is a small numerical value for F_{25}(LUMO)*. These values are obtained by shifting upwards the MO energy making it less reactive, i.e. making a bad electron acceptor. The suggests that atom 25 can participate in an electrostatic interaction with a negatively charged center or in a classical hydrogen bond, N-H….X. The substitution of H25 by a methyl group can help to clarify more the role of this atom. Atom 22 is the saturated carbon atom bonded to C20 (Fig. 6). Table 7 shows that all local MOs have a sigma nature. A high D_2 receptor affinity is associated with small numerical values for F_{22}(LUMO+1)*. If we agree that the same behavior is valid for F_{22}(LUMO)*, then this atom will behave like a bad electron acceptor. Table 7 shows that $(LUMO)_{22}^{*}$ is actually very distant from the molecular LUMO. On the other hand, $(HOMO)_{22}^{*}$ coincides with the molecular HOMO in the majority of cases and with the molecular (HOMO-1) in the remaining ones. Therefore, atom 22 seems to be involved in an alkyl, σ-π or alkyl-π interactions. Atom 22 is a good target to replace the methyl group by ethyl, n-propyl, or isopropyl substituents. Atom 10 is a sp^2 carbon atom belonging to rings B and C (Fig. 6). Table 6 shows that $(HOMO)_{10}^{*}$ has a pi character and coincides with the molecular HOMO in all cases. $(LUMO)_{10}^{*}$ has also a pi character and in all but one case it coincides with the molecular LUMO (the other case coincides with the molecular (LUMO+1)). A high D_2 receptor affinity is associated with small numerical values for S_{10}^{N}(LUMO+2)*. Small values, as was explained before, are obtained by shifting the MO energy to higher values, making this MO less reactive. If this condition is applied also to $(LUMO+1)_{10}^{*}$ and $(LUMO)_{10}^{*}$, then it is logical to suggest that atom 10 is interacting with an electron-deficient center. The interactions could be π-π or π-cation. Atom 12 is a sp^2 carbon atom of ring C (Fig. 6). Table 6 shows that all local frontier MOs have a pi nature. $(LUMO)_{12}^{*}$ coincides with the molecular LUMO in all cases. In only one case $(HOMO)_{12}^{*}$ coincides with the molecular HOMO. A high receptor affinity is associated with large numerical values for F_{12}(HOMO)*. This suggests that the ideal situation is when the molecular HOMO is fully localized on atom 12. Therefore we suggest that this atom is interacting with an electron-deficient center. The interactions can be π-cation or π-π. It is interesting to note that atoms 10 and 12, belonging to the same ring, interact in the same way with an unknown counterpart. If this is correct, then it is possible that they interact with a unique aromatic moiety through a π-π interaction. All the suggestions are displayed in the partial 2D pharmacophore of Fig. 15.

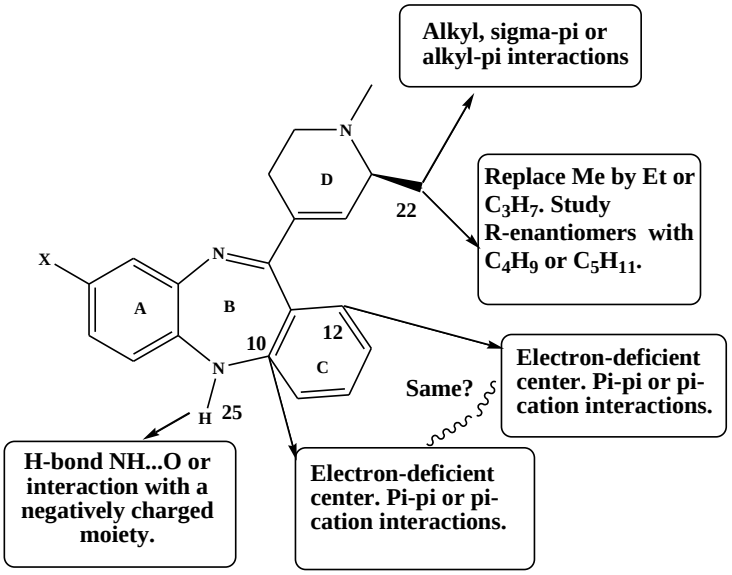

Figure 15: Partial 2D pharmacophore for D_2 receptor affinity

In summary, we have found statistically significant relationships relating the electronic structure of the (S)-enantiomers of a group of 11-(1,6-dimethyl-1,2,3,6-tetrahydropyridin-4-yl)-5H-dibenzo[b,e][1,4]diazepines to their dopamine D_1 and D_2 receptors affinities. In the case of the D_1 receptor four atoms were detected as being involved in the drug-receptor interaction. Three of them can be directly substituted to modify affinity. In the case of the D_2 receptor, four atoms were detected as participating in the interactions with the receptor. Three of them can be substituted to modify activity. In both receptors, the nitrogen atom N11 seems to be involved in hydrogen-bond interactions.

References

[1]. Tsuang, M. T.; Faraone, S. V.; Glatt, S. J. *Schizophrenia: the facts*. Oxford Univerity Press: Oxford, 2019.

[2]. Smart, S.; Kępińska, A.; Murray, R.; MacCabe, J. Predictors of treatment resistant schizophrenia: a systematic review of prospective observational studies. *Psychological medicine* **2021,** 51, 44-53.

[3]. Siskind, D.; Orr, S.; Sinha, S.; Yu, O.; Brijball, B.; Warren, N.; MacCabe, J. H.; Smart, S. E.; Kisely, S. Rates of treatment-resistant schizophrenia from first-episode cohorts: systematic review and meta-analysis. *The British Journal of Psychiatry* **2021**, 1-6.

[4]. Iwata, Y.; Nakajima, S.; Plitman, E.; Truong, P.; Bani-Fatemi, A.; Caravaggio, F.; Kim, J.; Shah, P.; Mar, W.; Chavez, S. Glutathione Levels and Glutathione-Glutamate Correlation in Patients With Treatment-Resistant Schizophrenia. *Schizophrenia Bulletin Open* **2021,** 2, sgab006.

[5]. Horne, C. M.; Vanes, L. D.; Verneuil, T.; Mouchlianitis, E.; Szentgyorgyi, T.; Averbeck, B.; Leech, R.; Moran, R. J.; Shergill, S. S. Cognitive control network connectivity differentially disrupted in treatment resistant schizophrenia. *NeuroImage: Clinical* **2021,** 30, 102631.

[6]. Hannon, E.; Dempster, E. L.; Mansell, G.; Burrage, J.; Bass, N.; Bohlken, M. M.; Corvin, A.; Curtis, C. J.; Dempster, D.; Di Forti, M. DNA methylation meta-analysis reveals cellular alterations in psychosis and markers of treatment-resistant schizophrenia. *Elife* **2021,** 10, e58430.

[7]. Campana, M.; Falkai, P.; Siskind, D.; Hasan, A.; Wagner, E. Characteristics and definitions of ultra-treatment-resistant schizophrenia–A systematic review and meta-analysis. *Schizophrenia Research* **2021,** 228, 218-226.

[8]. Verma, M.; Grover, S.; Chakrabarti, S. Effectiveness of clozapine on quality of life and functioning in patients with treatment-resistant schizophrenia. *Nordic Journal of Psychiatry* **2021,** 75, 135-144.

[9]. Kim, D. D.; Barr, A. M.; Stewart, S. E.; White, R. F.; Honer, W. G.; Procyshyn, R. M. Relationship between clozapine dose and severity of obsessive-compulsive symptoms. *Medical Hypotheses* **2021,** 148, 110506.

[10]. Citrome, L.; Volavka, J. Specific anti-hostility effects of atypical antipsychotics in persons with schizophrenia: from clozapine to cariprazine. *Harvard review of psychiatry* **2021,** 29, 20-34.

[11]. Albitar, O.; Harun, S. N.; Zainal, H.; Ibrahim, B.; Sheikh Ghadzi, S. M. Population pharmacokinetics of clozapine: a systematic review. *BioMed research international* **2020,** 2020.

[12]. Khokhar, J. Y.; Henricks, A. M.; Sullivan, E. D.; Green, A. I. Unique effects of clozapine: a pharmacological perspective. *Advances in pharmacology* **2018,** 82, 137-162.

[13]. Nakata, Y.; Kanahara, N.; Kimura, H.; Watanabe, H.; Iyo, M. Efficacy of clozapine on dopamine supersensitivity psychosis in schizophrenia. *International clinical psychopharmacology* **2017,** 32, 169-173.

[14]. Robichon, K.; Sondhauss, S.; Jordan, T. W.; Keyzers, R. A.; Connor, B.; La Flamme, A. C. Localisation of clozapine during experimental autoimmune encephalomyelitis and its impact on dopamine and its receptors. *Scientific reports* **2021,** 11, 1-13.

[15]. Nair, P. C.; McKinnon, R. A.; Miners, J. O.; Bastiampillai, T. Binding of clozapine to the GABA B receptor: Clinical and structural insights. *Molecular psychiatry* **2020,** 25, 1910-1919.

[16]. Hirjak, D.; Northoff, G.; Taylor, S. F.; Wolf, R. C. GABA B receptor, clozapine, and catatonia—a complex triad. *Molecular psychiatry* **2020**, 1-2.

[17]. Kim, D. D.; Barr, A. M.; Honer, W. G.; Procyshyn, R. M. Reversal of dopamine supersensitivity as a mechanism of action of clozapine. *Psychotherapy and psychosomatics* **2018,** 87, 306-308.

[18]. Kim, E.; Howes, O. D.; Veronese, M.; Beck, K.; Seo, S.; Park, J. W.; Lee, J. S.; Lee, Y.-S.; Kwon, J. S. Presynaptic dopamine capacity in patients with treatment-resistant schizophrenia taking clozapine: an [18 F] DOPA PET study. *Neuropsychopharmacology* **2017,** 42, 941-950.

[19]. McRobb, F. M.; Crosby, I. T.; Yuriev, E.; Lane, J. R.; Capuano, B. Homobivalent ligands of the atypical antipsychotic clozapine: design, synthesis, and pharmacological evaluation. *Journal of medicinal chemistry* **2012,** 55, 1622-1634.

[20]. Capuano, B.; Crosby, I. T.; McRobb, F. M.; Podloucka, A.; Taylor, D. A.; Vom, A.; Yuriev, E. The Synthesis and Preliminary Pharmacological Evaluation of a Series of Substituted 4′-Phenoxypropyl Analogues of the Atypical Antipsychotic Clozapine. *Australian journal of chemistry* **2010,** 63, 116-124.

[21]. Garipelli, N.; Reddy, B. M.; Jithan, A. Synthesis and evaluation of clozapine and its related compounds. *International Journal of Pharmaceutical Sciences and Nanotechnology* **2009,** 2, 762-767.

[22]. Capuano, B.; Crosby, I. T.; Lloyd, E. J.; Podloucka, A.; Taylor, D. A. Synthesis and Preliminary Pharmacological Evaluation of 4′-Arylalkyl Analogues of Clozapine. IV.* The Effects of Aromaticity and Isosteric Replacement. *Australian journal of chemistry* **2009,** 61, 930-940.

[23]. Capuano, B.; Crosby, I. T.; Lloyd, E. J.; Podloucka, A.; Taylor, D. A. Synthesis and Preliminary Pharmacological Evaluation of 4′-Arylalkyl Analogues of Clozapine. IV.* The Effects of Aromaticity and Isosteric Replacement. *Australian journal of chemistry* **2008,** 61, 930-940.

[24]. Capuano, B.; Crosby, I. T.; Lloyd, E. J.; Taylor, D. A. Synthesis and preliminary pharmacological evaluation of 4′-arylalkyl analogues of clozapine. III. Replacement of the tricyclic nucleus with a bicyclic template. *Australian journal of chemistry* **2007,** 60, 928-933.

[25]. Capuano, B.; Crosby, I. T.; Lloyd, E. J.; Neve, J. E.; Taylor, D. A. Aminimides as potential CNS acting agents. I. Design, synthesis, and receptor binding of 4′-aryl aminimide analogues of clozapine as prospective novel antipsychotics. *Australian journal of chemistry* **2007,** 60, 673-684.

[26]. Hussenether, T.; Hübner, H.; Gmeiner, P.; Troschütz, R. Clozapine derived 2, 3-dihydro-1H-1, 4-and 1, 5-benzodiazepines with D4 receptor selectivity: synthesis and biological testing. *Bioorganic & medicinal chemistry* **2004,** 12, 2625-2637.

[27]. Capuano, B.; Crosby, I. T.; Lloyd, E. J.; Podloucka, A.; Taylor, D. A. Synthesis and preliminary pharmacological evaluation of 4′-arylalkyl analogues of clozapine. II. Effect of the nature and length of the linker. *Australian journal of chemistry* **2003,** 56, 875-886.

[28]. Capuano, B.; Crosby, I. T.; Lloyd, E. J.; Taylor, D. A. Synthesis and Preliminary Pharmacological Evaluation of 4´-Arylmethyl Analogues of Clozapine. I. The Effect of Aromatic Substituents. *Australian journal of chemistry* **2002,** 55, 565-576.

[29]. Asproni, B.; Pau, A.; Bitti, M.; Melosu, M.; Cerri, R.; Dazzi, L.; Seu, E.; Maciocco, E.; Sanna, E.; Busonero, F. Synthesis and pharmacological evaluation of 1-[(1, 2-diphenyl-1 H-4-imidazolyl) methyl]-4-phenylpiperazines with clozapine-like mixed activities at dopamine D2, serotonin, and GABAA receptors. *Journal of medicinal chemistry* **2002,** 45, 4655-4668.

[30]. Watanabe, H.; Ishida, K.; Yamamoto, M.; Horiguchi, M.; Isobe, Y. Synthesis and pharmacological evaluation of 11-(1, 6-dimethyl-1, 2, 3, 6-tetrahydropyridin-4-yl)-5H-dibenzo [b, e][1, 4] diazepines with clozapine-like receptor occupancy at dopamine D1/D2 receptor. *Bioorganic & Medicinal Chemistry Letters* **2020,** 30, 127563.

[31]. The results presented here are obtained from what is now a routinary procedure. For this reason, all papers have a similar general structure. This model contains *standard* phrases for the presentation of the methods, calculations and results because they do not need to be rewritten repeatedly and because the number of possible variations to use is finite. See: Hall, S., Moskovitz, C., and Pemberton, M. 2021. Understanding Text Recycling: A Guide for Researchers. Text Recycling Research Project. Online at textrecycling.org. In.

[32]. Gómez Jeria, J. S. La Pharmacologie Quantique. *Bollettino Chimico Farmaceutico* **1982,** 121, 619-625.
[33]. Gómez-Jeria, J. S. On some problems in quantum pharmacology I. The partition functions. *International Journal of Quantum Chemistry* **1983,** 23, 1969-1972.
[34]. Gómez-Jeria, J. S. The use of competitive ligand binding results in QSAR studies. *Il Farmaco; edizione scientifica* **1985,** 40, 299-302.
[35]. Gómez-Jeria, J. S. Modeling the Drug-Receptor Interaction in Quantum Pharmacology. In *Molecules in Physics, Chemistry, and Biology*, Maruani, J., Ed. Springer Netherlands: 1989; Vol. 4, pp 215-231.
[36]. Gómez-Jeria, J. S.; Ojeda-Vergara, M. Parametrization of the orientational effects in the drug-receptor interaction. *Journal of the Chilean Chemical Society* **2003,** 48, 119-124.
[37]. Barahona-Urbina, C.; Nuñez-Gonzalez, S.; Gómez-Jeria, J. S. Model-based quantum-chemical study of the uptake of some polychlorinated pollutant compounds by Zucchini subspecies. *Journal of the Chilean Chemical Society* **2012,** 57, 1497-1503.
[38]. Bruna-Larenas, T.; Gómez-Jeria, J. S. A DFT and Semiempirical Model-Based Study of Opioid Receptor Affinity and Selectivity in a Group of Molecules with a Morphine Structural Core. *International Journal of Medicinal Chemistry* **2012,** 2012 Article ID 682495, 1-16.
[39]. Gómez-Jeria, J. S. *Elements of Molecular Electronic Pharmacology (in Spanish)*. 1st ed.; Ediciones Sokar: Santiago de Chile, 2013; p 104.
[40]. Gómez-Jeria, J. S. A New Set of Local Reactivity Indices within the Hartree-Fock-Roothaan and Density Functional Theory Frameworks. *Canadian Chemical Transactions* **2013,** 1, 25-55.
[41]. Gómez-Jeria, J. S.; Flores-Catalán, M. Quantum-chemical modeling of the relationships between molecular structure and in vitro multi-step, multimechanistic drug effects. HIV-1 replication inhibition and inhibition of cell proliferation as examples. *Canadian Chemical Transactions* **2013,** 1, 215-237.
[42]. Paz de la Vega, A.; Alarcón, D. A.; Gómez-Jeria, J. S. Quantum Chemical Study of the Relationships between Electronic Structure and Pharmacokinetic Profile, Inhibitory Strength toward Hepatitis C virus NS5B Polymerase and HCV replicons of indole-based compounds. *Journal of the Chilean Chemical Society* **2013,** 58, 1842-1851.
[43]. Gómez-Jeria, J. S.; Kpotin, G. Some Remarks on The Interpretation of The Local Atomic Reactivity Indices Within the Klopman-Peradejordi-Gómez (KPG) Method. I. Theoretical Analysis. *Research Journal of Pharmaceutical, Biological and Chemical Sciences* **2018,** 9, 550-561.
[44]. Gómez-Jeria, J. S. 45 Years of the KPG Method: A Tribute to Federico Peradejordi. *Journal of Computational Methods in Molecular Design* **2017,** 7, 17-37.
[45]. Frisch, M. J.; Trucks, G. W.; Schlegel, H. B.; Scuseria, G. E.; Robb, M. A.; Cheeseman, J. R.; Scalmani, G.; Barone, V.; Petersson, G. A.; Nakatsuji, H.; Li, X.; Caricato, M.; Marenich, A. V.; Bloino, J.; Janesko, B. G.; Gomperts, R.; Mennucci, B.; Hratchian, H. P. *Gaussian 16 16Rev. A.03*, Gaussian: Pittsburgh, PA, USA, 2016.
[46]. Gómez-Jeria, J. S. *D-Cent-QSAR: A program to generate Local Atomic Reactivity Indices from Gaussian16 log files*, v. 1.0; Santiago, Chile, 2020.
[47]. Gómez-Jeria, J. S. An empirical way to correct some drawbacks of Mulliken Population Analysis (Erratum in: J. Chil. Chem. Soc., 55, 4, IX, 2010). *Journal of the Chilean Chemical Society* **2009,** 54, 482-485.
[48]. Statsoft. *Statistica v. 8.0*, 2300 East 14 th St. Tulsa, OK 74104, USA, 1984-2007.
[49]. Gómez-Jeria, J. S.; Robles-Navarro, A.; Kpotin, G.; Garrido-Sáez, N.; Gatica-Díaz, N. Some remarks about the relationships between the common skeleton concept within the Klopman-Peradejordi-Gómez QSAR method and the weak molecule-site interactions. *Chemistry Research Journal* **2020,** 5, 32-52.